

Synthesis and structural characterization of a new chiral macrocycle derived from α,α' -(bistrifluoromethyl)-9,10-anthracendimethanol and terephthalic acid

Martina Palomino-Schätzlein · Kepa K. Burusco ·
Teodor Parella · Albert Virgili · Carlos Jaime

Received: 20 January 2009 / Accepted: 14 April 2009 / Published online: 30 April 2009
© Springer Science+Business Media B.V. 2009

Abstract The synthesis and the structural properties of a chiral macrocyclic cyclooctatetracontaphane host are reported. The macrocycle is obtained by cyclization of six molecules of terephthalic acid and six molecules of enantiopure α,α' -(bistrifluoromethyl)-9,10-anthracendimethanol. The latter is known for its enantioselective interaction with different organic molecules and is used as effective chiral solvating agent for pharmaceutical mixtures. Experimental NMR diffusion data of the chiral macrocycle reveal a predominant conformation in solution with a cavity, suitable for host–guest interactions. This result is confirmed by theoretical calculations using molecular dynamics.

Keywords Enantiorecognition · Molecular dynamics · Diffusion · Aromatic

The design and synthesis of artificial receptors is a central element in supramolecular chemistry to understand the

fundamental principles of molecular recognition. Macrocycles are the largest group of synthetic receptors studied due to their special ability to form host–guest complexes, and they are extensively applied in highly diverse areas of chemistry and biochemistry [1–12].

Besides the relatively strong and often dominant hydrogen bonding, ion pairing, and hydrophobic effects in aqueous media, the arene–arene interactions seem to be particularly important for the formation of supramolecular complexes when aromatic rings are present [13]. Thus, macrocycles consisting of a cavity surrounded by several aromatic residues have proven to be highly versatile receptors for aromatic guests [14, 15].

On the other hand, chiral macrocycles are also of special interest as they are capable of selectively binding enantiomers, imitating molecular recognition in biological systems. A variety of chiral macrocycles have been synthesized and studied for their enantiomeric recognition abilities [16–22]. However, most of these cycles are relatively small and as the diameter of the ring becomes larger, the macrocycle becomes more flexible and host–guest interactions are more difficult [23]. To prevent a collapse of large-volume structures, the backbone must be made of rigid components, usually aromatic segments.

In this context, we report here the synthesis of the symmetric macrocycle **1** (Fig. 1) consisting of 6 units of terephthalic acid and of α,α' -(bistrifluoromethyl)-9,10-anthracendimethanol **2**. The special ability of **2** in complexing selectively with chiral organic aromatic compounds has been shown by recent studies [24]. Furthermore, the aromatic components of **1** will help the macrocycle to remain rigid and we expect **1** to have interesting host–guest complexing properties.

M. Palomino-Schätzlein (✉)
Servicio de Resonancia Magnética Nuclear,
Centro de Investigación Príncipe Felipe,
46012 Valencia, Spain
e-mail: mpalomino@cipf.es

K. K. Burusco · A. Virgili · C. Jaime
Departament de Química, Universitat Autònoma
de Barcelona, 08193 Bellaterra, Spain

T. Parella
Servei de RMN, Universitat Autònoma de Barcelona, 08193
Bellaterra, Spain

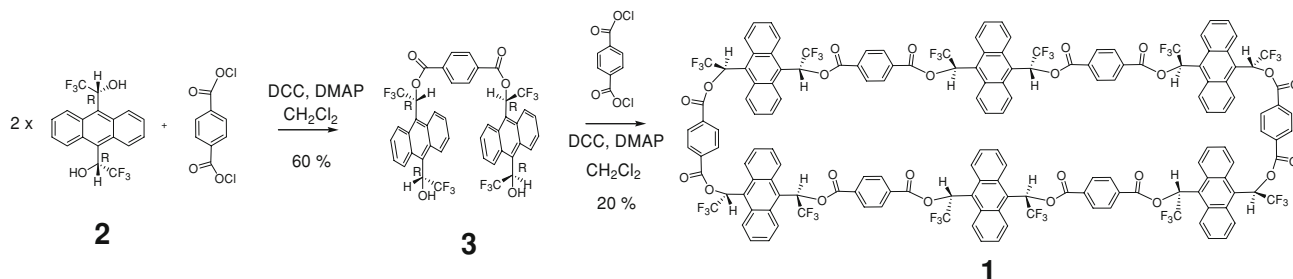


Fig. 1 Synthesis of Macrocycle **1**

Experimental section

Synthesis of di-<{(R,R)-1-[10-(1-hidroxy-2,2,2-trifluoroethyl)-9-anthryl]-2,2,2-trifluoroethoxy}terephthalate **3**

Terephthaloyl chloride (271 mg, 1.3 mmol) was added to a solution of (*R,R*)- α,α' -(bistrifluoromethyl)-9,10-antracenedimethanol **2** (1.00 g, 2.7 mmol), Et₃N (0.5 ml, 3.2 mmol) and DMAP (33 mg, 0.3 mmol) in anhydrous CH₂Cl₂ (150 ml) under nitrogen. The reaction mixture was stirred for 2 hours at ambient temperature and then treated with 1 M HCl (120 ml), 1 M NaHCO₃ (120 ml) and a saturated solution of NaCl (120 ml). The organic phase was dried over MgSO₄ and the volatiles were removed under reduced pressure. Purification of the product using silica gel flash chromatography (eluent EtOAc/hexane, 10:1) gave diester (*R,R,R,R*)-**3** (700 mg, 60%) as a white solid: mp 202–210°C; $[\alpha]_D^{20} +160$ (*c*1.0, CHCl₃); IR (ATR) cm⁻¹: 3250, 1738, 1258, 1178, 1128, 1087, 1026, 867, 763, 723, 644; ¹H NMR (500 MHz, acetone-d₆, 250 K) δ (*cisoid*): 9.34 (d, $J_{8c,7c}$ = 9.28 Hz, 1H, H_{8c}), 9.05 (d, $J_{8c,7c}$ = 9.01 Hz, 1H, H_{8c}), 8.80 (d, $J_{1c,2c}$ = 9.2 Hz, 1H, H_{1c}), 8.55 (d, $J_{1c,2c}$ = 9.2 Hz, 1H, H_{1c}), 8.41 (s, 4H, H₁₄), 8.29 (q, $J_{11c,F}$ = 8.1 Hz, 1H, H_{11c}), 7.84 (dd, $J_{2c,7c}$ = 9.2 Hz, $J_{2c,1c}$ = 9.2 Hz, 1H, H_{2c}), 7.73 (dd, $J_{7c,2c}$ = 9.1 Hz, $J_{7c,8c}$ = 9.0 Hz, 1H, H_{7c}), 7.7 (dd, $J_{7c,2c}$ = 9.2 Hz, $J_{7c,8c}$ = 9.3 Hz, 1H, H_{7c}), 7.68 (dd, $J_{2c,7c}$ = 9.1 Hz, $J_{2c,1c}$ = 9.2 Hz, 1H, H_{2c}), 7.11 (m, 2H, H_{OH}), 6.68 (q, $J_{11c,F}$ = 8.3 Hz, 1H, H_{11c}) δ (*transoid*): 9.29 (d, $J_{8t,7t}$ = 9.28 Hz, 1H, H_{8t}), 9.04 (d, $J_{8t,7t}$ = 8.84 Hz, 1H, H_{8t}), 8.89 (d, $J_{1t,2t}$ = 9.1 Hz, 1H, H_{1t}), 8.65 (d, $J_{1t,2t}$ = 9.1 Hz, 1H, H_{1t}), 8.41 (s, 4H, H₁₄), 8.34 (q, $J_{11t,F}$ = 8.1 Hz, 1H, H_{11t}), 7.87 (dd, $J_{2t,2t}$ = 9.1 Hz, $J_{2t,1t}$ = 9.1 Hz, 1H, H_{2t}), 7.78 (dd, $J_{2t,2t}$ = 9.1 Hz, $J_{2t,1t}$ = 9.1 Hz, 1H, H_{2t}), 7.71 (dd, $J_{7t,7t}$ = 9.2 Hz, $J_{7t,8t}$ = 8.8 Hz, 1H, H_{7t}), 7.58 (dd, $J_{7t,7t}$ = 9.2 Hz, $J_{7t,8t}$ = 9.3 Hz, 1H, H_{7t}), 7.11 (m, 2H, H_{OH}), 7.04 (qt, $J_{11t,F}$ = $J_{11t,OH}$ = 8.6 Hz, 1H, H_{11t}); ¹³C NMR (500 MHz, acetone-d₆, 250 K) δ (*cisoid*): 163.09 (C_{12c}), 162.97 (C_{12t}), 132.74 (C_{13c}), 132.72 (C_{13t}), 131.78,

131.10, 131.01, 130.81 (C_{1'ac}, C_{8'ac}, C_{1'at} i C_{8'at}), 130.66, 130.53, 130.33, 129.67 (C_{10c}, C_{10'c}, C_{10t} and C_{10't}), 129.22, 129.12, 129.08, 128.99 (CF_{3c}, CF_{3'c}, CF_{3t} and CF_{3't}), 130.20 (C₁₄), 128.86 (C_{8'c}), 128.68 (C_{8't}), 127.25 (C_{2c}), 126.98 (C_{2t}), 126.43 (C_{7c}), 126.37 (C_{7t}), 126.23 (C_{8c}), 126.08 (C_{8t}), 125.67 (C_{2'}), 124.74 (C_{7'c}), 124.53 (C_{7't}), 124.15 (C_{1't}), 124.12, 123.94, 123.29, 123.16 (C_{1ac}, C_{8ac}, C_{1at} and C_{8at}), 123.91 (C_{1c}), 123.70 (C_{1t}), 122.87 (C_{1c}), 70.37 (C_{11c} i C_{11t}), 68.83 (C_{11'c}), 68.61 (C_{11't}). MALDI-TOF (THF-cca), m/z, %: 878 (M, 44), 522 (16), 423 (16), 399 (16), 356 (100).

Synthesis of macrocycle **1**

Terephthaloyl chloride (162 mg, 0.8 mmol) dissolved in anhydrous CH₂Cl₂ (50 ml) was added drop-wise to a solution of di-<{(R,R)-1-[10-(1-hidroxy-2,2,2-trifluoroethyl)-9-anthryl]-2,2,2-trifluoroethoxy}terephthalate **3** (700 mg, 0.8 mmol), Et₃N (0.12 ml, 0.8 mmol) and DMAP (20 mg, 0.16 mmol) in anhydrous CH₂Cl₂ (250 ml) under nitrogen. The reaction mixture was stirred for 5 hours at ambient temperature and then treated with 1 M HCl (120 ml), 1 M NaHCO₃ (120 ml) and a saturated solution of NaCl (120 ml). The organic phase was dried over MgSO₄ and the volatiles were removed under reduced pressure. Purification of the product using silica gel flash chromatography (CH₂Cl₂/hexane, 1:3) gave macrocycle **1** (160 mg, 20%) as a white solid: mp 270–275 °C; $[\alpha]_D^{20} +180$ (*c*1.0, CHCl₃); IR (ATR) cm⁻¹: 3054, 2360, 1740, 1264, 1234, 1185, 1134, 1091, 1016, 895, 736, 705. ¹H NMR (500 MHz, acetone-d₆, 298 K) δ : 9.09 (m, 6H, H_{8t}), 9.03 (m, 6H, H_{8c}), 8.91 (m, 6H, H_{1t}), 8.82 (m, 6H, H_{1c}), 8.36 (m, 12H, H₁₁), 8.35 (s, 24 H, H₁₄), 7.84 (m, 12H, H_{2t} i H_{2c}), 7.73 (m, 12H, H_{7t} i H_{7c}); ¹³C NMR (500 MHz, acetone-d₆, 298 K) δ : 164.0 (C₁₂), 133.7 (C₁₃), 132.4, 131.9, 131.2, 130.8 (C_{1ac}, C_{8at}, C_{1at} i C_{8ac}), 131.2 (C₁₄), 129.6 (CF₃), 128.5 (C_{7c} i C_{7t}), 127.5 (C_{8c} i C_{8t}), 126.8, 126.5 (C_{2c} i C_{2t}), 124.8, 124.5 (C_{1c} i C_{1t}), 124.0 (C₉), 71.0 (C_{11c} i C_{11t}); MALDI-TOF (THF-cca), m/z, %: 3024.9 (M, 44), 2520 (60), 2012 (60).

Diffusion

The measurement of D was made using bipolar-gradient LED pulse sequence [25], using $\Delta = 0.2$ s and $\delta = 0.001$ s. For each experiment, sine-shaped pulsed-field gradients were incremented from 2 to 95% of the maximum strength in 16 spaced steps. The temperature regulation system eurotherm VT-3000 supplied by the manufacturer was used and maximum oscillations of ± 0.2 K were permitted. Sample spinning of 20 Hz was used for minimizing convection effects [26].

Computational calculations

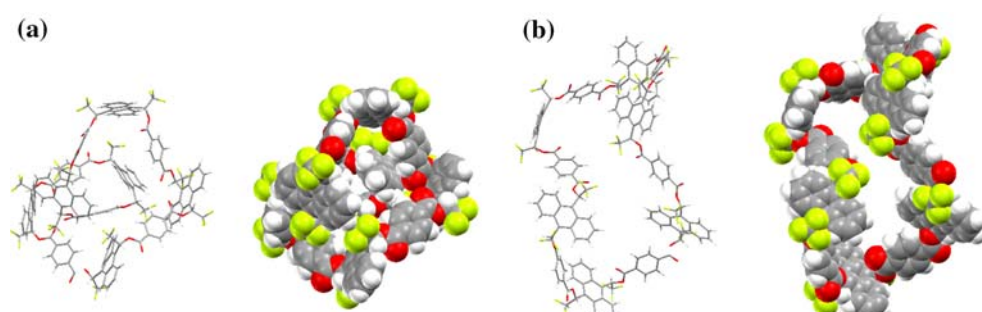
All molecular dynamics calculations were realized with AMBER 7 [27, 28], using the parm99 [29] force field and the solvent simulations were carried out in chloroform. SHAKE [30, 31] procedures were used to limit the stretching of all atoms and the degree of thermal coupling was varied to avoid a blow up. The geometric minimization conditions were the standard from Amber 7. A maximum of 10,000 steps and 2 minimizations methods were selected: the first 10 steps are done by the Steepest Descent Method [32] and than the Conjugated Gradient Method [33–35] is used to reach convergence. Molecular dynamics of the macrocycle where done in 2 steps: a) heating and equilibration and b) sampling of the system in equilibrium.

Results and discussion

Chiral macrocycle **1** was prepared via a two-step sequence starting from commercial enantiopure α,α' -(bistrifluoromethyl)-9,10-anthracenedimethanol **2** and terephthaloyl chloride. The first step was for diester **3** to be formed (Fig. 1) in 60% yield employing standard esterification conditions.

The isolated diester reacted with another equivalent of terephthaloyl chloride forming a mixture of different polymeric compounds from where macrocycle **1** was easily separated by column chromatography in 20% yield. The mass of the macrocycle was confirmed by Maldi-ToF Mass Spectroscopy.

Fig. 2 Structures and surfaces of **1** obtained by Molecular Mechanics calculations under different conditions. **a** in vacuum **b** in CHCl_3



A conformational analysis of the macromolecule using molecular dynamics simulations (AMBER 7 [27, 28] with the parm99 force field [29]) was performed to get a better idea of the geometry of the cycle. The calculations were carried out first in vacuum and than in the presence of solvent molecules (CHCl_3), obtaining a different result for each case. In vacuum, the cycle adopts a completely folded conformation, enhanced by intramolecular hydrogen bonding and π -stacking interactions (Fig. 2).

On the other hand, in the presence of a non-protic solvent, different low-energy unfolded conformations were found, leaving an open cavity for host–guest interactions. Cavity sizes were comprised between 700 and 990 \AA^3 , and the dimension of the cavity changed between $20 \times 10 \text{\AA}$ (biggest) and $14 \times 10 \text{\AA}$ (smallest).

Figure 3 shows the superimposed structures from the molecular dynamics simulation, and it is clear that in the presence of solvent, macrocycle **1** becomes more flexible, but without folding.

In order to further validate these results and study the properties of the macrocycle in solution, we used NMR Diffusion Spectroscopy [36, 37] that has been successfully used in supramolecular organic chemistry [38]. Diffusion coefficients (D) are experimentally determined by monitoring the signal intensity decay in a pulsed-field gradient spin-echo experiment spectrum as a function of the overall

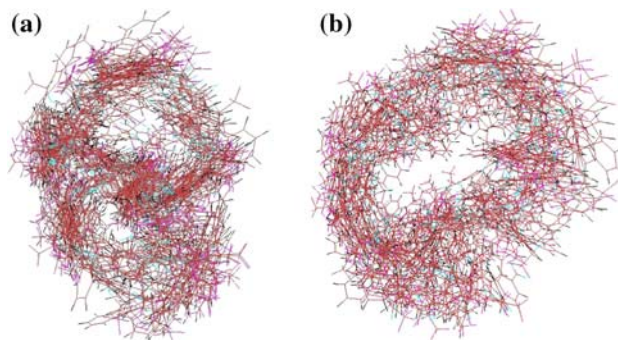
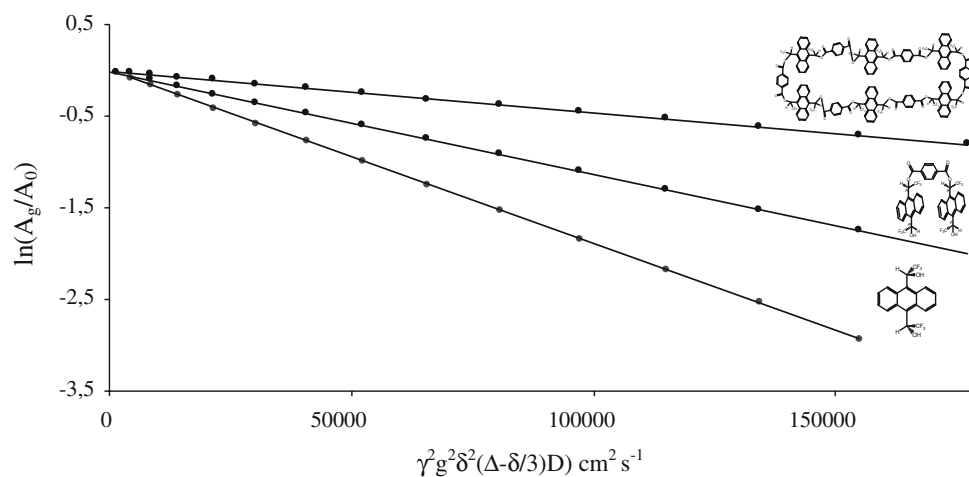


Fig. 3 Representation of the superimposition of 50 structures of macrocycle **1** obtained from molecular dynamics simulation **a** in vacuum **b** in CHCl_3

Fig. 4 Plot of $\ln(A_g/A_0)$ versus $\gamma^2 g^2 \delta^2(\Delta - \delta/3)D$ for compounds **1**, **2** and **3**



gradient strength [39]. The experimental D values can be related to molecular constraints such as molecular size, molecular weight, and hydrodynamic radius.

In a diffusion NMR experiment using sinusoidal shaped gradients, the signal intensity of a given resonance decays as given in Equation [1]

$$A_g = A_0 \exp(-\gamma^2 g^2 \delta^2(\Delta - \delta/3)D) \quad (1)$$

where A_g and A_0 are the signal intensities in the presence and absence of pulsed-field gradients (PFG), respectively, γ is the gyromagnetic ratio (rad s G^{-1}), g is the strength of the diffusion gradients (G cm^{-1}), D is the diffusion coefficient of the observed spins ($\text{cm}^2 \text{s}^{-1}$), δ is the length of the diffusion gradients (s), and Δ is the time separation between the leading edges of the two diffusion pulsed gradients (s) [40]. Diffusion coefficients were obtained by measuring the slope in the following relationship:

$$\ln(A_g/A_0) = -\gamma^2 g^2 \delta^2(\Delta - \delta/3)D \quad (2)$$

Diffusion coefficients (D) of macrocycle **1**, and of the parent compounds **2** and **3** were experimentally measured

under identical conditions (Fig. 4). As expected, D decreases as the size of the molecule increases, owing to the fact that large molecules move slower in solution.

The Stokes–Einstein equation allows us to relate the D values to the corresponding hydrodynamic radius. The theoretical radii of gyration of **1**, **3** and **2**, obtained from the low energy conformations in presence of solvent, are 15 Å, 7 Å and 4 Å, respectively (Table 1).

Assuming that temperature and viscosity remain invariable in all experiments, the following relationship between the diffusion coefficients and the hydrodynamic radius of the three molecules can be established: $D_1:D_3:D_2 = 1/R_1:1/R_2:1/R_3$. From the diffusion coefficients displayed in Table 1, the experimental relationship between the radius $R_1:R_3:R_2$ is 4:1.7:1 which is in strong agreement with the theoretical 3.8:1.8:1 ratio. The experimental hydrodynamic radius of macrocycle **1** is four times the hydrodynamic radius of **2**. In vacuum, on the other hand, the radius of **1** is much smaller, and the theoretical relationship is completely different (2.4:1.8:1) discarding the presence of a folded conformation in solution.

Conclusion

The coherence between computational calculations in solution and the experimental data confirms the hypothesis that macrocycle **1** adopts a non-folded conformation with an open cavity. This is an interesting result as it means that we have managed to synthesize a large macrocycle, with an available cavity, but with enough flexibility to adapt to guest molecules.

Furthermore, the chirality of **1** (with 12 defined chiral centres) will allow enantiodiscrimination between both enantiomers of a chiral guest molecule.

Table 1 ^1H NMR Diffusion data and hydrodynamic radii values (r_H in Å) for compounds **1**, **3** and **2**

Compound	Diffusion coefficient ($10^{-10} \text{ m}^2 \text{s}^{-1}$) ^a	r_H (Å) from NMR data ^b	r_H (Å) from calculations ^c
1	4.70	15.3	15
3	10.2	7.06	7
2	18.7	3.85	4

^a Data measured in Acetone at 298 K. Concentrations of 0.05 mM

^b Data calculated using the Stokes–Einstein equation. η (Acetone, 298 K) = $0.303 \times 10^{-3} \text{ kg s}^{-1} \text{ m}^{-1}$

^c Values of the most stable conformations in solution

Annex 1

Diffusion: See the appendix Table 2, 3 and 4

Table 2 Values of g and $\gamma^2 g^2 \delta^2(\Delta-\delta/3)$ for compounds 2

Experiment	Strength of diffusion gradients (g)	$\gamma^2 g^2 \delta^2(\Delta-\delta/3)$	Signal intensity ($\delta = 8,67$ ppm)
1	0,674	78,53	214,5746
2	2,765	1321,66	213,7294
3	4,855	4074,80	200,7061
4	6,945	8338,21	184,5815
5	9,036	14114,99	164,4865
6	11,126	21399,64	143,3871
7	13,217	30199,10	121,2314
8	15,307	40504,98	99,8751
9	17,397	52321,12	79,9188
10	19,488	65654,25	61,9353
11	21,578	80491,62	46,9448
12	23,668	96839,25	34,0704
13	25,759	114706,04	24,4555
14	27,849	134074,90	17,3272
15	29,939	154954,02	11,5199
16	32,030	177354,48	7,7654

Table 3 Values of g and $\gamma^2 g^2 \delta^2(\Delta-\delta/3)$ for compounds 3

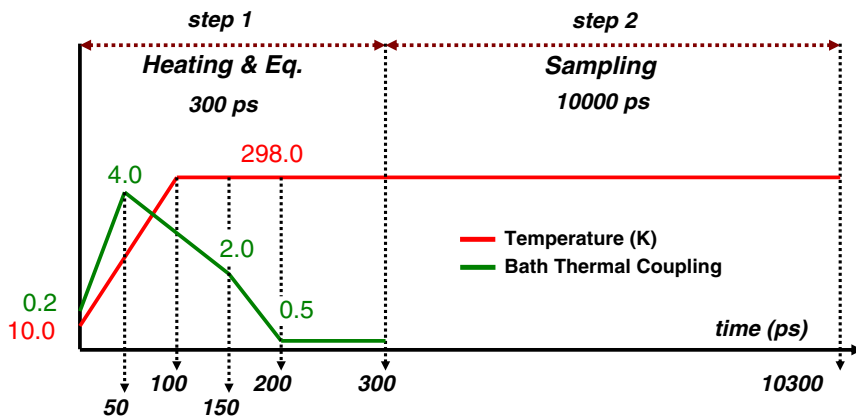
Experiment	Strength of diffusion gradients (g)	$\gamma^2 g^2 \delta^2(\Delta-\delta/3)$	Signal intensity ($\delta = 8,67$ ppm)
1	0,674	78,53	715,3909
2	2,765	1321,66	753,8437
3	6,945	8338,21	649,5893
4	9,036	14114,99	602,8789
5	11,126	21399,64	552,0041
6	13,217	30199,10	505,5622
7	15,307	40504,98	447,5732
8	17,397	52321,12	392,2835
9	19,488	65654,25	342,1704
10	21,578	80491,62	288,963
11	23,668	96839,25	239,9443
12	25,759	114706,04	195,5539
13	27,849	134074,90	157,5443
14	29,939	154954,02	125,829
15	32,030	177354,48	98,2659

Table 4 Values of g and $\gamma^2 g^2 \delta^2 (\Delta - \delta/3)$ for compounds **1**

Experiment	Strength of diffusion gradients (g)	$\gamma^2 g^2 \delta^2 (\Delta - \delta/3)$	Signal intensity ($\delta = 8.67$ ppm)	Signal intensity ($\delta = 8.36$ ppm)	Signal intensity ($\delta = 7.81$ ppm)
1	0,674	296,3363	32,7664	296,3363	109,6733
2	2,765	292,5985	33,5346	292,5985	108,707
3	4,855	290,0837	33,1142	290,0837	107,3444
4	6,945	286,3626	32,4379	286,3626	105,8546
5	9,036	277,0492	31,4335	277,0492	103,0839
6	11,126	268,0691	30,4438	268,0691	99,8341
7	13,217	257,4807	29,0458	257,4807	95,4924
8	15,307	245,5003	27,4715	245,5003	91,6728
9	17,397	232,2519	26,3949	232,2519	86,8885
10	19,488	218,2984	24,685	218,2984	82,274
11	21,578	204,206	22,9651	204,206	76,9197
12	23,668	189,5428	21,2114	189,5428	71,0719
13	25,759	175,234	19,7203	175,234	66,2777
14	27,849	160,6754	17,6063	160,6754	60,9078
15	29,939	146,507	16,2151	146,507	55,4869
16	32,030	132,7056	14,6673	132,7056	50,6187

Annex 2. Details of computational calculations**1. Geometric optimizations in vacuum**

```
Minmizations in vacuum &cntrl
  imin=1,      nmropt=0,
  ntx=1,      irest=0,   ntrx=1,
  ntb=0,      igb=0,     nsnb=25,
  ipol=0,      gbsa=0,
  dielc=1.0,   cut=12.0, intdiel=1.0,
  scnb=2.0,    scee=1.2,
  ibelly=0,    ntr=0,
  maxcyc=10000,
&end
```

2. Molecular dynamics of the macrocycle

Step 1:

```

Molecular dynamics in vacuum. Heating and equilibration
&cntrl
imin=0,          nmropt=1,
ntx=1,           irest=0,      ntrx=1,
ntxo=1,           ntp=1000,    ntwr=1000,
iwrap=0,          ntwx=1000,   ntwv=0,   ntwe=1000,
lastrst=3000000,
ioutfm=0,         ntwprt=0,   idecomp=0,
ntf=2,            ntb=0,       igb=0,   nsnb=25,
ipol=0,           gbsa=0,
dielc=1.0,        cut=12.0,   intdiel=1.0,
scnb=2.0,          scee=1.2,
nstlim=300000,   nscm=1000,  nrespa=1,
t=0.0,            dt=0.001,   vlimit=10.0,
ig=71277,         ntt=1,      vrnd=0,
temp0=298.0,     tempi=0.0,   heat=0.0,
dtemp=5.0,        tautp=0.5,
ntc=2,            tol=0.00001
&end
&wt type='TEMP0', istep1=1,      istep2=100000, value1=10.0,   value2=298.0, &end
&wt type='TEMP0', istep1=100001, istep2=300000, value1=298.0,   value2=298.0, &end
&wt type='TAUTP', istep1=1,      istep2=50000,  value1=0.2,    value2=4.0,   &end
&wt type='TAUTP', istep1=50001, istep2=150000, value1=4.0,   value2=2.0,   &end
&wt type='TAUTP', istep1=150001, istep2=200000, value1=2.0,   value2=0.5,   &end
&wt type='TAUTP', istep1=200001, istep2=300000, value1=0.5,   value2=0.5,   &end
&wt type='REST',  istep1=1,      istep2=50000,  value1=0.1,   value2=1.0,   &end
&wt type='REST',  istep1=50001, istep2=250000, value1=1.0,   value2=1.0,   &end
&wt type='REST',  istep1=250001, istep2=300000, value1=1.0,   value2=0.1,   &end
&wt type='END'
&end

```

Step 2:

```

Molecular dynamics in vacuum. Sampling.
&cntrl
imin=0,          nmropt=0,
ntx=5,           irest=1,      ntrx=1,
ntxo=1,           ntp=10000,   ntwr=10000,
iwrap=0,          ntwx=10000,  ntwv=0,   ntwe=10000,
lastrst=3000000,
ioutfm=0,         ntwprt=0,   idecomp=0,
ntf=2,            ntb=0,       igb=0,   nsnb=25,
ipol=0,           gbsa=0,
dielc=1.0,        cut=12.0,   intdiel=1.0,
scnb=2.0,          scee=1.2,
nstlim=10000000,   nscm=1000,  nrespa=1,
t=0.0,            dt=0.001,   vlimit=10.0,
ig=71277,         ntt=1,      vrnd=0,
temp0=298.0,     tempi=298.0, heat=0.0,
dtemp=5.0,        tautp=0.5,
ntc=2,            tol=0.00001,
&end

```

References

- Karhanov, E.E., Maksimov, A.L., Runova, E.A., Kardasheva, Y.S., Terenina, M.V., Buchneva, T.S., Guchkova, A.Y.: Supramolecular catalytic systems based on calixarenes and cyclodextrins. *Macromol. Symp.* **204**, 159–174 (2003)
- Gibson, S.: Amino acid derived macrocycles: an area driven by synthesis or application? *Angew. Chem. Int. Ed.* **45**, 1364–1377 (2006)
- Wenz, G., Han, B.-H., Müller, A.: Cyclodextrin rotaxanes and polyrotaxanes. *Chem. Rev.* **106**, 782–817 (2006)
- Fürstner, A.: Total Syntheses and biological assessment of macrocyclic glycolipids. *Eur. J. Org. Chem.* **2004**(5), 943–958 (2004)
- Sieber, S.A., Marahiel, M.A.: Learning from nature's drug factories: nonribosomal synthesis of macrocyclic peptides. *J. Bacteriol.* **185**, 7036–7043 (2003)
- Sandford, G.: Macrocycles from perhalogenated heterocycles. *Chem. Eur. J.* **9**, 1464–1469 (2003)
- Radecka-Paryzek, W., Patroniak, V., Lisowski, J.: Metal complexes of polyaza and polyoxaaza Schiff base macrocycles. *Coord. Chem. Rev.* **249**, 2156–2175 (2005)
- Kawase, T.: Allenophane and allenoacetylenic macrocycles: a new class of chiral cyclophanes. *Angew. Chem. Int. Ed.* **44**, 7334–7336 (2005)
- Agrawal, Y. K., Bhatt, H.: Calixarenes and their biomimetic applications. *Bioinorg. Chem. Appl.* **2**, 237–274 (2004)

10. Easton, C.J.: Calixarenes and their biomimetic applications. *Pure Appl. Chem.* **77**, 1865–1871 (2005)
11. Moyer, B.A., Birdwell, J.F., Bonnesen, P.V., Delmau, L.H.: Use of macrocycles in nuclear-waste cleanup: a real-world application of a calixcrown in technology for the separation of cesium. *Macrocycl. Chem.* **38**, 3–405 (2005)
12. Lamb, J. D., Gardner, J. S.: Application of macrocyclic ligands to analytical chromatography. In: Gloe, K. (ed.) *Macrocyclic Chemistry*, pp. 349–363. Springer, Netherlands (2005)
13. Klärner, F.-G., Burkert, U., Kamieth, M., Boese, R., Benet-Buchholz, J.: Molecular tweezers as synthetic receptors: molecular recognition of electron-deficient aromatic and aliphatic substrates. *Chem. Eur. J.* **5**, 1700–1707 (1999)
14. Meyer, E.A., Castellano, R.K., Diederich, F.: Interactions with aromatic rings in chemical and biological recognition. *Angew. Chem. Int. Ed.* **42**, 1210–1250 (2003)
15. Hunter, C.A., Lawson, K., Perkins, J., Urch, C.J.: Aromatic interactions. *J. Chem. Soc. Perkin Trans. 2*, 651–669 (2001)
16. Zhang, X.X., Bradshaw, J.S., Izatt, R.M.: Enantiomeric recognition of amine compounds by chiral macrocyclic receptors. *Chem. Rev.* **97**, 3313–3361 (1997)
17. Wenzel, T., Wilcox, J.D.: Chiral reagents for the determination of enantiomeric excess and absolute configuration using NMR spectroscopy. *Chirality* **15**, 256–270 (2003)
18. Ward, T.J., Farris, A.B.: Chiral separations using the macrocyclic antibiotics: a review. *J. Chromatogr. A* **906**, 73–89 (2001)
19. Xiao, T.L., Armstrong, D.W.: Enantiomeric separations by HPLC using macrocyclic glycopeptide-based chiral stationary phases, an overview. *Methods Mol. Biol.* **243**, 113–171 (2004)
20. Shahgaldian, P., Pieles, U.: Cyclodextrin derivatives as chiral supramolecular receptors for enantioselective sensing. *Sensors* **6**, 593–615 (2006)
21. Kuhn, R., Riester, D., Fleckenstein, B., Wiesmüller, K.-H.: Evaluation of an optically active crown ether for the chiral separation of di- and tripeptides. *J. Chromatogr. A* **716**, 371–379 (1995)
22. Esquivel, B., Nicholson, L., Peerey, L., Fazio, M.: High performance liquid chromatographic separation of dipeptide and tripeptide enantiomers using a chiral crown ether stationary phase. *J. High Resolut. Chromatogr.* **14**, 816–823 (1991)
23. Höger, S.: Highly efficient methods for the preparation of shape-persistent macrocyclics. *J. Polym. Sci. Part A: Polym. Chem.* **37**, 2685–2698 (1999)
24. Pomares, M., Sánchez-Ferrando, F., Virgili, A., Alvarez-Larena, A., Piniella, J.F.: Preparation and structural study of the enantiomers of alfa, alfa-Bis(trifluoromethyl)-9, 10-anthracenedimethanol and its perdeuterated isotopomer, highly effective chiral solvating agents. *J. Org. Chem.* **67**, 753–758 (2002)
25. Wu, D., Chen, A., Johnson, C.S.: An improved diffusion ordered spectroscopy experiment incorporating bipolar gradient pulses. *J. Magn. Reson.* **115**, 260–264 (1995)
26. Esturau, N., Sanchez-Ferrando, F., Gavin, J.A., Roumestand, C., Delsuc, M., Parella, T.: The use of sample rotation for minimizing convection effects in self-diffusion NMR measurements. *J. Magn. Reson.* **153**, 48–55 (2001)
27. Case, D.A., Pearlman, D.A., Caldwell, J.W., Cheatham, T.E III., Wang, J., Ross, W.S., Simmerling, C.L., Darden, T.A., Merz, K.M., Stanton, R.V., Cheng, A.L., Vincent, J.J., Crowley, M., Tsui, V., Gohlke, H., Radmer, R.J., Duan, Y., Pitera, J., Massova, I., Seibel, G.L., Singh, U.C., Weiner, P.K., Kollman, P.A.: AMBER 7. University of California, San Francisco (2002)
28. Pearlman, D.A., Case, D.A., Caldwell, J.W., Ross, W.S., Cheatham, T.E III., DeBolt, S., Ferguson, D., Seibel, G., Kollman, P.: AMBER a package of computer programs for applying molecular mechanics, molecular dynamics and free energy calculations to stimulate the structural and energetic properties of molecules. *Comp. Phys. Commun.* **91**(1–3), 1–41 (1995)
29. Wang, J., Cieplak, P., Kollman, P.A.: How well does a restrained electrostatic potential (RESP) model perform in calculating conformational energies of organic and biological molecules? *J. Comput. Chem.* **21**(12), 1049–1074 (2000)
30. Ryckaert, J.P., Ciccotti, G., Berendsen, H.J.C.: Numerical-integration of Cartesian equations of motion of a system with constraints—molecular-dynamics of N-alkanes. *J. Comput. Phys.* **23**(3), 327–341 (1977)
31. Ryckaert, J.P.: Special geometrical constraints in the molecular-dynamics of chain molecules. *Mol. Phys.* **55**(3), 549–556 (1985)
32. Snyman, J.A.: Practical mathematical optimization: an introduction to basic optimization theory and classical and new gradient-based algorithms. Springer, Berlin, Heidelberg (2005) ISBN 0-387-24348-8
33. Hestenes, M.R., Stiefel, E.: Methods of conjugate gradients for solving linear systems. *J. Res. Natl. Bur. Stand.* **49**(6), 409–436 (1952)
34. Polak, E., Ribiére, G.: Note sur la convergence de directions conjuguées. *Rev. Francaise Informat. Recherche Opérationnelle*. 3e Année 16, 35–43 (1969)
35. Fletcher, R., Reeves, C.M.: Function minimization by conjugate gradients. *Comput. J.* **7**(2), 149–154 (1964)
36. Johnson, C.S.: Diffusion ordered nuclear magnetic resonance spectroscopy: principles, applications. *Progr. NMR Spectrosc.* **34**, 203–256 (1999)
37. Price, W.S.: Pulsed-field gradient NMR as a tool for studying translational diffusion. Part II. experimental aspects. *Conc. Magn. Reson.* **10**, 197–237 (1998)
38. Brand, T., Cabrita, E.J., Berger, S.: Intermolecular interaction as investigated by NOE and diffusion studies. *Prog. NMR Spec.* **46**, 159–196 (2005)
39. Stejskal, E.O., Tanner, J.E.: Diffusion measurements: spin echoes in the presence of a time-dependent field gradient. *J. Chem. Phys.* **42**, 288–292 (1965)
40. Price, W.S.: Pulsed-field gradient nuclear magnetic resonance as a tool for studying translational diffusion: Part 1. basic theory. *Concepts Magn. Reson.* **9**, 299 (1997)